12th International Congress on the Deterioration and Conservation of Stone
Columbia University, New York, 2012

EFFECT OF SPRAYING FERROCYANIDE IONS ON NACL CONTAMINATED SAMPLES

Sonia Gupta[1], Leo Pel[1] and Alison Heritage[2]

[1]Eindhoven University of Technology, Department of Applied Physics, Den Dolech 2, 5600 MB Eindhoven, The Netherlands (email:sgupta@tue.nl, l.pel@tue.nl)
[2]International Centre for the Study of the Preservation and Restoration of Cultural Property (ICCROM), Via di San Michele 13, 00153 Rome, Italy

Abstract

Salt weathering leads to destruction of many valuable cultural heritage monuments. To reduce the impact of destruction, effective treatment methods are required. The use of crystallisation inhibitors to mitigate salt damage has been proposed in the past, however to date the effectiveness and safety of their application on cultural heritage objects has not been proven. Therefore, a detailed experimental study is performed to see the effect of spraying potassium hexa-cyanoferrate (II) tri-hydrate inhibitor on NaCl contaminated samples. We focus on the concentration levels reached by NaCl solutions within porous media during drying, and the associated water and ion transport processes taking place.

Two types of drying experiments were performed (1) droplet drying experiments, and, (2) salt contaminated brick drying experiments. For droplet drying experiments the salt solution droplets with and without inhibitor were dried. In brick drying experiments salt contaminated materials were sprayed with inhibitor solution and dried afterwards. From droplet drying experiments it is shown that in the presence of inhibitor higher supersaturation is achieved and supersaturation increases with increase in inhibitor concentration. Also, a change in crystal morphology from cubic to dendritic crystals is seen. Dendritic crystals occupy much larger surface area compared to cubic crystals. The spreading effect increases with increase in inhibitor concentration. From the brick drying experiments it is shown that in the presence of inhibitor, due to the dendritic crystal morphology, advection becomes the governing phenomenon for ion transport. It results in the transport of the salt ions to the outer surface of the brick, where it crystallises in the form of non-destructive efflorescence. No higher supersaturation is observed within the materials sprayed with inhibitor solution. These results show that ferrocyanide ions could potentially be affective against NaCl damage.

Keywords: salt weathering, NaCl, ferrocyanide ions, drying

1. Introduction

Soluble salts such as chlorides, sulphates and nitrates are widely recognized as a cause of destruction in porous building materials, mainly due to crystallisation inside the porous matrix. The growth of salt crystals exerts pressure on the pore walls, which can exceed the tensile strength of the material thus leading to damage (Scherer 1999). Among various salts present inside the porous material sodium chloride (NaCl) is one of the most damaging salt. The source of salt can be ground water, flooding, rain and also chemical composition of the material itself. It is well known that the deterioration occurs

DRAFT

only if the salt crystals deposits within the pores of the material often known as sub-florescence. This happens when migration of the salt solution to the surface is slower than the evaporation of the solution from the surface. On the other hand, when salt crystallises on the external surface of the material it is known as efflorescence. Efflorescence is unsightly but in most cases not harmful for the materials. Different methods have been tested in the past to control salt damage but with varying degree of success. Recently, the use of crystallisation inhibitors has been proposed as a potential preventive treatment method. For bulk solutions, increased supersaturation levels in the presence of inhibitor have been reported in the past (Navarro 2002). However, to our knowledge, to date no study has been published regarding the effect of these compounds on the concentration of NaCl solutions inside a porous media. This indeed is a very important aspect for salt damage. As it is known that the process behind the damage due to salt crystallisation is the growth of salt crystals in confined spaces (e.g. pores), hence exerting crystallisation pressure on the pore walls. Thermodynamically, the crystallisation pressure can be related to supersaturation (C/C_o) of the solution by the well-known Corren's equation (Correns 1949):

$$P_C = \frac{RT}{V_m} \ln \frac{C}{C_o}$$

Where P_c is the crystallisation pressure, R is the universal gas constant, T is the absolute temperature, V_m is the molar volume of the salt crystal, C and C_o are increasing concentration in vicinity of crystal and saturation concentration of salt respectively. Before using inhibitors to treat historic objects detailed experimental studies are required to assess the effectiveness and safety of their application. In the past, a detailed study was performed to test the effectiveness of ferrocyanide ions as inhibitor against NaCl damage (Gupta 2012 submitted). For this study, the sample materials were initially saturated with salt and inhibitor solution. However, in practice for the monuments already contaminated with salt the only way to test the effectiveness of inhibitors is by spraying inhibitor solution on the contaminated walls. Therefore, in this work a systematic study has been undertaken to see the effect of spraying hexa-cyanoferrate (II) ions as inhibitor on the salt contaminated walls. We focused on the concentration levels reached by NaCl solutions within porous media during drying and the associated water and ion transport processes taking place. This behavior is not completely understood, because it is not easy to measure non-destructively the concentration of ions inside a porous material during dynamic experiments. However, with the help of a specially designed Nuclear Magnetic Resonance set-up (Pel 1995) we were able to non-destructively measure both hydrogen and sodium ions simultaneously during drying experiments.

2. Nuclear Magnetic Resonance (NMR)

In this study Nuclear Magnetic Resonance (NMR) is used for carrying out non-destructive, quantitative and simultaneous measurement of both hydrogen and sodium ion content in a sample. NMR is based on the principle that in a magnetic field, nuclei have a specific resonance frequency and can be excited by a radio frequency field. The resonance frequency *f* (Hz) depends linearly on the magnitude of the magnetic field:

$$f = \frac{\gamma}{2\pi} B_0$$

DRAFT

Where $\gamma/2\pi$ (HzT^{-1}) is the gyromagnetic ratio, B_0 (T) is the main magnetic field. For ^1H $\gamma/2\pi$ is 42.58 $MHzT^{-1}$ and ^{23}Na is 11.26 $MHzT^{-1}$. Therefore, by using a specific frequency the method can be made sensitive to a particular type of nucleus, in this case either hydrogen or sodium. The signal intensity S of a spin echo as used in the experiment is given by:

$$S = k\rho\left[1-\exp\left(-\frac{T_r}{T_1}\right)\exp\left(-\frac{T_e}{T_2}\right)\right]$$

Where S is signal intensity, k is the sensitivity of the nuclei relative to hydrogen, ρ is the density of the nuclei, T_r and T_1 are the repetition time of the pulse sequence and spin-lattice relaxation time, T_e and T_2 are the spin echo time and spin-spin relaxation time. To measure the maximum signal, i.e. from all pore sizes, T_e should be as short as possible as T_1 and T_2 are proportional to the pore size. As the sensitivity of ^{23}Na nuclei is low relative to hydrogen (k_H = 1, k_{Na} = 0.1), 256 averages of the spin echo measurements are taken for Na nuclei relative to eight averages of hydrogen thereby giving the possibility to obtain sufficient signal to noise ratio. Since the relaxation time for Na in NaCl crystals is of order of 10 µs (Pel 2003) only dissolved Na ions are measured using the NMR set-up. For the presented experiments, a home-built NMR scanner with a static magnetic field of 0.78 T and gradient up to 0.3 T/m is used. To perform quantitative measurements a Faraday shield is placed between the coil and the sample (Pel 1995).

3. Droplet drying experiments

In the beginning, a series of droplet drying experiments was performed to observe the crystallisation behavior of NaCl salt solution droplets with and without crystallisation inhibitor. The aim behind this study was to see the influence of increasing inhibitor concentration on NaCl supersaturation, crystal morphology and also to find out the optimum inhibitor concentration for spray drying experiments.

3.1. Experimental set-up

A schematic of the setup is shown in Figure 1. A quartz sample holder with inner diameter of 20 mm was used. Droplets of 300 µl salt solution (3 m NaCl) with and without inhibitor were dried using 0 per cent relative humidity and about 1 l min^{-1} air flow rate.

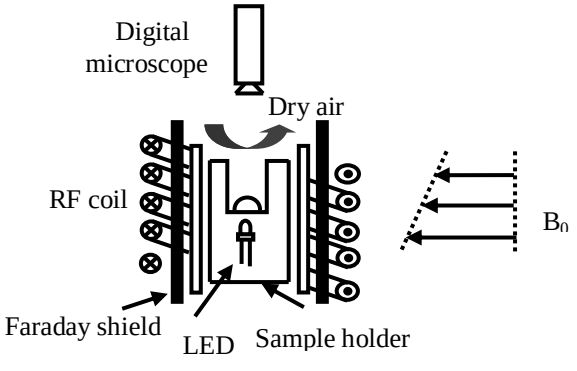

DRAFT

Figure 1. A schematic diagram of the NMR set-up used for droplet drying experiments

The effect of increased inhibitor concentration on the nucleation and crystal morphology of NaCl was studied. Time lapse microscopy of the crystallisation was performed using a dino-lite digital microscope. Four LED's were placed below the substrate as a lighting source for imaging within the NMR setup. The capture of photomicrograph images along with the NMR measurements gives the possibility to visualize the drying of the droplet while simultaneously obtaining information about NaCl concentration within the droplets. NMR is used to measure hydrogen (H) and sodium (Na) and from their ratio (Na/H) the concentration of dissolved sodium ions in the droplet is calculated. As we are doing simultaneous time lapse microscopy, we can see exactly at what concentration the salt crystal appears. Thus, we can relate the onset of crystallisation with the Na concentration in a droplet. The supersaturation is calculated as C/C_o where C and C_o are increasing concentration in vicinity of crystal and saturation concentration (6.1 mol/kg of water) of NaCl respectively.

3.2. Results

Initially, we started with drying of a salt solution droplet with and without inhibitor. For salt solution droplet without inhibitor the onset of crystallisation was seen at a concentration of 6.2 ± 0.5 m giving a supersaturation of 1.06 ± 0.04 (see fig. 2). In the presence of inhibitor, the crystallisation was seen at a concentration higher than the saturation concentration of NaCl and thus the droplet supersaturates. The results are shown in Figure 2, where the supersaturation is plotted as a function of inhibitor concentration.

DRAFT

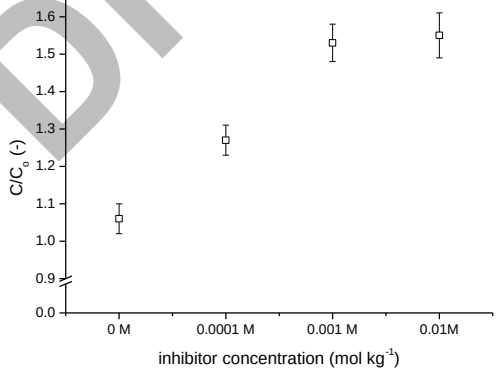

Figure 2. The figure shows the supersaturation plotted as a function of inhibitor concentration

As can be seen in Figure 2, supersaturation increases with increase in inhibitor concentration. We found a maximum supersaturation up to 1.55 m in the presence of 0.01 m inhibitor. In addition, due to the presence of inhibitor NaCl crystal morphology changes from cubic crystal morphology to dendritic crystal morphology. The pictures showing NaCl crystal morphology at the end of drying experiment are shown in Figure

3. In case of drying of a NaCl solution droplet without inhibitor, cubic crystals were seen growing at the liquid/air interface. Whereas, in the presence of inhibitor dendritic crystals first forms at the liquid/air interface. These crystals then spread very rapidly all over the substrate. Spreading of the crystals was more at higher inhibitor concentration. The branches of dendritic crystals provide a pathway for spreading of solution to much larger surface area. This phenomenon is commonly known as 'salt creep' (see also Figure 3).

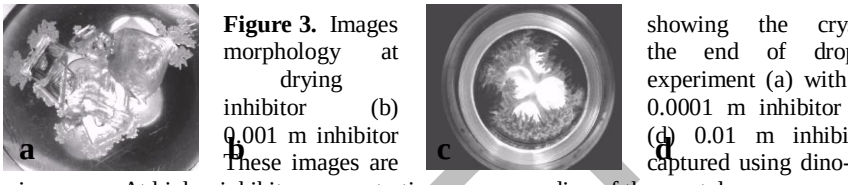

Figure 3. Images showing the crystal morphology at the end of droplet drying experiment (a) with no inhibitor (b) 0.0001 m inhibitor (c) 0.001 m inhibitor (d) 0.01 m inhibitor. These images are captured using dino-lite digital microscope. At higher inhibitor concentration more spreading of the crystals were seen.

Due to the enlarged surface area for evaporation at higher inhibitor concentration a similar increase in the drying rate was observed. So, at higher inhibitor concentration faster drying was seen.

4. Brick drying experiment

4.1 Materials

The materials used in this study were fired-clay brick and Granada limestone. The red fired-clay brick is of a type typically used for construction in the Netherlands, and had an average porosity (as measured by water immersion method) of 0.32 $m^3 m^{-3}$, and a pore size distribution ranging from 1-10 µm (accounting for ~ 80 per cent of the total pore space), as determined by Mercury Intrusion Porosimetry (MIP). The Granada limestone is a buff colored stone commonly used as a building material in Granada, Spain. In this stone calcite is the main component (90 wt%), together with lesser amounts of SiO_2 and Al_2O_3. This material has an average porosity (as measured by water immersion method) of 0.29 $m^3 m^{-3}$, and a bimodal pore size distribution with pores ranging from 0.3-1 µm (40 per cent) and 1-100 µm (60 per cent) as determined by MIP. In this study potassium hexa-cyanoferrate (II) tri-hydrate $K_4[Fe(CN)_6]\cdot 3H_2O$ was tested as a crystallisation inhibitor.

4.2 Experimental set-up

A schematic diagram of the brick drying experiments is given in Figure 4. The cylindrical samples 20 mm in diameter and 40 mm in length were vacuum saturated with salt solution (3 m NaCl). In order to have homogenous distribution of the salt crystals inside the samples, the saturated samples were freeze dried for approx. 10 days. For freeze drying, the samples were initially immersed in liquid nitrogen at temperature -196 ^oC. This causes immediate freezing of the salt solution inside the material. After that the frozen samples were placed in an ultra-high vacuum at 10^{-2} mb for about 8-10

DRAFT

days. This causes direct sublimation of the solid water to water vapor thus leaving behind the salt crystals at their initial place. The sample weight was monitored after every 24 h. After about 7-8 days the sample attains constant weight indicating complete absence of water. In this way salt contaminated samples were prepared. Afterwards, the contaminated samples were sprayed with inhibitor solution prepared in water. For spraying 0.01 m inhibitor solution was used.

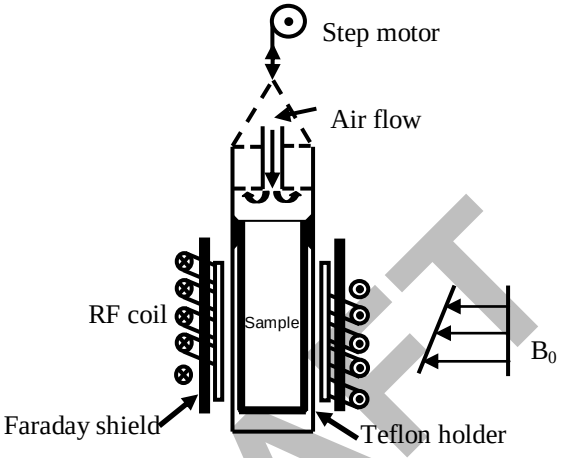

Figure 4. A schematic diagram of the NMR set-up used for spray drying experiments

This is due to the fact that maximum effect of inhibitor on supersaturation and crystal morphology was seen at this concentration. To avoid evaporation of water after spraying the samples were covered in an aluminum foil and were placed inside a sealed polythene bag for about 4 h. The procedure of spraying inhibitor and covering the contaminated sample was repeated for about 2 days. The aim behind doing so was to give sufficient time to inhibitor to penetrate inside the material through diffusion. First order approximation about the timescales of diffusion was made using $x = \sqrt{2Dt}$ where x (m) is the length, D (m^2 s^{-1}) is the diffusion coefficient of the salt ions and t (s) is the time. After that the prepared samples were sealed using Teflon tape from all sides except from the top surface and placed inside the NMR sample chamber. Samples were exposed to dry air with a flow 1 l min^{-1} and 0 per cent relative humidity, thereby creating one-dimensional drying experiment. The sample position was moved in the vertical direction using a step motor to allow measurement of the H and Na content throughout the sample length. Measuring one drying profile takes about 3 hours, while the complete drying experiment takes in the order of a few days depending on the composition of the salt solution. Therefore, small variations in the moisture and ion profiles during a single scan can be neglected. After each drying experiment was completed the efflorescence formed on the top of the sample was collected and weighed.

4.3 Results

DRAFT

In the previous section we have shown that the presence of inhibitor significantly increases the supersaturation within the salt solution droplets. As explained earlier higher supersaturation can cause higher crystallisation pressure and hence the risk of damage is then greater. Therefore, to ascertain the effects of inhibitor on NaCl ion transport and crystallisation behavior within porous media, a series of one dimensional drying experiment were performed. In the past a detailed study was performed where ferrocyanide ions were tested as an inhibitor against NaCl damage. For this study the materials were initially saturated with salt and inhibitor solution. The results show that in the presence of inhibitor most of the salt crystallises as non-destructive efflorescence (Gupta 2012, submitted). However, in practice for the materials that are already contaminated with salt the only way to test inhibitor is by spraying inhibitor solution on the contaminated walls. So, laboratory experiments were performed to simulate practical situation. The measured moisture profiles and the calculated concentration profiles for fired-clay brick are given in figure 5a and 5b and for Granada limestone are given in Figures 5c and 5d respectively. The recurrent irregularities in the profiles are the result of inhomogenities of the sample. For both materials, two drying stages can be observed i.e. externally limited and internally limited shown by a vertical and a horizontal arrow in Figures 5a and 5c.

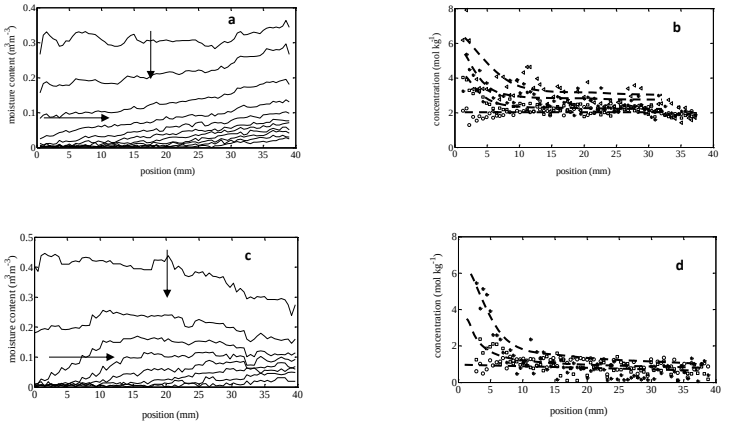

Figure 5. The measured moisture profiles (a) the corresponding concentration profiles (b) for fired-clay brick and the measured moisture profiles (c) the corresponding concentration profiles (d) for Granada limestone plotted as a function of position during drying. The samples were intially contaminated with salt and then sprayed with 0.01 m ihibitor solution and dried using dry air with flow 1 l min^{-1} and 0% relative humidity. The profiles are given for every 3 h. The drying surface is at 0 mm. The dotted lines in the concentration profiles are guide to the eye.

The first 2-3 profiles in both the samples are almost flat representing the first drying stage. During this stage there is continuous capillary flow of water to the surface and drying is limited by external conditions such as relative humidity and air flow. Afterwards, the drying front starts to recede below the sample surface, and the moisture profiles are no longer flat. This represents the second drying stage where the

continuous capillary network of water breaks up to form liquid islands. During this stage drying occurs by vapor diffusion through the porous medium, in response to the relative humidity gradient between the vicinity of the liquid island and the drying surface (Hall 2002). The transition point between these two drying stages can be identified as critical moisture content. Critical moisture content was observed to be near 0.08 m^3m^{-3} in both the samples. In Figure 4b the initial concentration of NaCl is 2 m, whereas the sample material was initially vacuum saturated with 3 m NaCl solution. The lower concentration of salt is due to the fact that after freeze drying the sample was sprayed with inhibitor solution. It was not possible to reach the same saturation level as was done initially by vacuum saturation. Due to this all the crystallised salt inside the material was not dissolved and thus the concentration of NaCl was lesser than the initial concentration of 3 m. During drying an increase in salt solution concentration is seen near the drying surface (see Figures 5b and 5d). This is due to the advection of salt ions along with the moisture towards the drying surface. This is confirmed by calculating the Peclet number. The Peclet number is dimensionless number that shows the competition between diffusion and advection and is given as (Huinink 2002):

$$P_e = \frac{|U|L}{D}$$

Where U (m s^{-1}) is the fluid velocity, L (m) is the length of the sample and D (m^2 s^{-1}) is the diffusion coefficient of salt ions in porous materials and taken equal to 1.3×10^{-9} m^2 s^{-1} (Veran-Tissoires 2012). Using measured moisture profiles the fluid velocity is calculated (Pel 2010). For Pe < 1, diffusion dominates and for P_e > 1, advection dominates. The calculated value of P_e ~ 5 in both the cases confirms that advection is the dominant phenomenon and causes salt crystallisation near the drying surface. Due to dendritic crystal morphology in the presence of inhibitor, the effective surface area for evaporation increases (Veran-Tissoires 2012). The salt solution creeps along the branches of the dendrites and transports more and more dissolved salt ions towards the drying surface which was seen as efflorescence by the end of drying experiment. This efflorescence was collected and weighed. The efflorescence formed in the spray experiments is compared with the efflorescence formed in the saturation experiment (in saturation experiments the samples were vacuum saturated with salt and inhibitor solution (Gupta 2012, submitted). The results are shown in Figure 6 where the efflorescence formed is plotted as a function of inhibitor concentration. As shown in Figure 6 the amount of efflorescence formed increases with increasing inhibitor concentration. This is due to more pronounced spreading of dendritic salt crystals at high inhibitor concentration. However, no supersaturation was seen within salt contaminated materials sprayed with inhibitors.

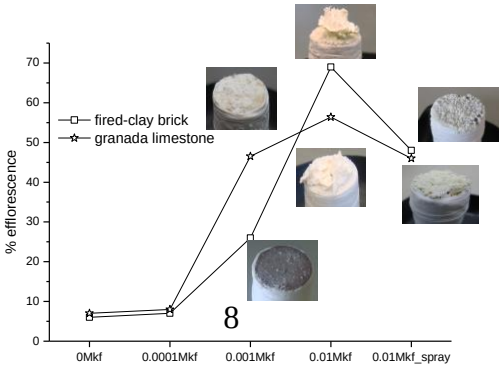

DRAFT

Figure 6. Figure shows the efflorescence formed at the end of drying plotted as a function of inhibitor concentration. With increasing inhibitor concentration the amount of salt crystallised as efflorescence also increases. Significant efflorescence is seen in spray drying experiments.

From the results it is concluded that spraying of inhibitor on salt contaminated materials helps to remove the salt as non-destructive efflorescence. However, it should be kept in mind that it is very important to give time to the inhibitor molecules to diffuse inside the material. In our case we did so by covering the material after spraying with inhibitor. This helped the inhibitor to diffuse inside the material and causes the crystallisation of salt as efflorescence. In a previous study done by Lubelli *et al*. this effect was not taken into account. This might be the reason that they did not observe much efflorescence in their experiments (Lubelli 2007). Regarding the action of inhibitor we concluded that the presence of inhibitor changes the drying conditions near the material/air interface due to the change in crystal morphology. The immediate crystallisation near the drying surface provides a sink for the salt ions and as a result most of the salt crystallises as non-destructive efflorescence.

5. Conclusions

From the droplet drying experiments it is concluded that in the presence of inhibitor higher supersaturation is attained. The supersaturation increases with increase in inhibitor concentration. NaCl crystal morphology changes from cubic to dendritic crystals. The branches of dendrite crystals provide much larger surface area for evaporation of the water and consequently make the drying process faster.

From the spray drying experiments it is concluded that it is important to give sufficient time to the inhibitor molecules to diffuse inside the contaminated material. In the presence of inhibitor the drying conditions changes near the material/air interface due to changes in crystal morphology. Dendrite crystals provide much larger surface area for evaporation and advection becomes the governing phenomenon throughout the drying process. Advection of dissolved salt ions causes crystallisation of salt near the drying surface as non-destructive efflorescence. This indicates that application of ferrocyanide ions on NaCl contaminated walls could potentially be affective against damage in building materials. However, at the same time it must be kept in mind that in practice there is not only the single salt present in the building materials but indeed mixture of salt is present. Therefore it is important to explore the effect of inhibitor on the mixture of salt. This will be studied in future work.

Acknowledgements

We thank Hans Dalderop and Jef Noijen for their technical assistance. A part of this project is supported by the Dutch technology foundation (STW). Special thanks to Carlos Rodriguez Navarro for providing the Granada limestone for study.

References

DRAFT

Correns, W. 1949. 'Growth and dissolution of crystals under linear pressure'. Faraday discussion, **5**: 267-271.

Gupta, S., Terheiden, K., Pel, L. *et al*. 2012. 'The influence of ferrocyanide inhibitors on the transport and crystallisation processes of sodium chloride in porous building materials'. Submitted in Journal of crystal Growth and Design.

Hall, C., Hoff, W.D. 2002. 'Water Transport in Brick, Stone and Concrete'. Spon Press, London. 188-194.

Huinink, H.P., Pel, L., Michels, M.A. 2002. 'How ions distribute in a drying porous medium: a simple model'. Physics of fluids, **14**: 1389-1395.

Lubelli, B., Van Hees, R.P.J. J. 2007. 'Effectiveness of crystallisation Inhibitors in preventing salt damage in building materials'. Journal of Cultural Heritage, **8**: 223-234.

Navarro, C.R., Fernandez, L.L., Doehne, E. *et al*. 2002. 'Effects of ferrocyanide ions on NaCl crystallisation in porous stone'. Journal of Crystal Growth, **243**: 503-516.

Pel, L. 1995. 'Moisture Transport in porous building materials'. Ph.D. thesis. Department f physics, Eindhoven University of Technology, The Netherlands.

Pel, L., Huinink, H., Kopinga, K. 2003. 'Salt transport and crystalllisation in porous building material'. Magnetic Resonance Imaging, **21**: 317-320.

Pel, L., Sawdy, A., Voronina, V. J. 2010. 'Physical principles and efficiency of salt extraction by poulticing'. Journal of Cultural Heritage, **11**: 59-67.

Scherer, G.W. 1999. 'Crystallisation in pores'. Cement and Concrete Research, **29**: 1347-1358.

Veran-Tissoires, S., Marcoux, M., Prat, M. 2012. 'Discrete salt crystallisation at the surface of a porous medium'. Physics Review Letters, **108**: 054502.

DRAFT